

Synthesis and Application of Nano-structured Bi-layer YSZ-LZ Thermal Barrier Coating

R.K. Satpathy^{*,§}, B.R. Mishra[#], B. Mallick[@], and B.K. Mishra[!]

^{*}DRDO-Defence Metallurgical Research Laboratory, Hyderabad - 500 058, India

[§]CSIR-Academy of Scientific and Innovative Research, Ghaziabad 201 002, India

[#]Indian Rare Earths Limited, Chatrapur - 761 045, India

[@]Hindustan Aeronautics Limited, Koraput-763 004, India

[!]Indian Institute of Technology, Goa - 403 401, India

^{*}E-mail: rk.satpathy@dmrl.drdo.in

ABSTRACT

Present work is on synthesis of high purity Nano-structured TBC materials, Lanthanum Zirconate and YSZ. They were prepared via wet chemical routes, starting from the indigenous source minerals such as zircon and monazite available in the beach sand. This is first time that the results of TBC materials synthesis from these base minerals, their purification and a high end application being presented comprehensively. Their characterisation and thermal barrier application on aeroengine components have been presented. The total oxide impurities being critical to the life of the coating, could be controlled within 0.03 per cent by weight. On comparison with other powders it was found that the indigenously synthesised YSZ powder had practically 100 per cent tetragonal prime phase and no monoclinic phase; whereas others had significant amounts of monoclinic phases present in them. Both YSZ and LZ powders were sinter agglomerated at 850 °C to preclude the possibility of any contamination and sieved. APS process was used to realise nano-structured bi-layer coating on the exhaust nozzle parts of an aeroengine. The components were subjected to rapid thermal transients during long accelerated endurance testing, equivalent to 1000 h of engine operations. The coatings also withstood the gas erosion of supersonic combustion products, vibratory loads of 4 g and more than 30000 nozzle actuations similar to aircraft manoeuvre. The paper also presents a brief review of implications of a nano-structured thermal barrier coating and certain nuances of chemical synthesis which forms the backbone of the strategies for durable coatings.

Keywords: Nano materials; Lanthanum Zirconate (LZ)-YSZ bilayer TBC; Aeroengine application; IR-Nano particles interaction; Ilmenite; Zircon; Monazite beach sand

1. INTRODUCTION

Currently 7-8 wt% Ytria stabilised Zirconia, with the maximum surface temperature capability of about 1200 °C is the industry standard for TBC material and has proved its worth for almost four decades. At higher temperatures, degradation of the coating takes place and changes in microstructure as well as mechanical properties result in reduced strain tolerance and a decrease in thermal fatigue life of the coating. On the other hand, Lanthanum Zirconate (LZ), with general formula $A_2B_2O_7$ (pyrochlore structure), possesses attractive intrinsic properties such as higher thermal and phase stability (close to 2000 °C), lower sintering tendency and thermal conductivity (k) compared to YSZ. Thus LZ has received significant attention in recent times¹⁻⁴. Among the pyrochlores, $La_2Zr_2O_7$ (LZ) seems to have great potential as a TBC material due to its excellent bulk properties vis-a-vis YSZ. But it has lower coefficient of thermal expansion and slightly higher specific gravity compared to YSZ. Though nano LZ can mitigate the problem to a certain extent, it can not be applied directly on

the MCrAlY bond coat. Therefore LZ is applied as a top coat material over YSZ for enhanced coating life. A nano-structured bi-layer is also expected to reflect certain amount of radiations thus providing a more effective TBC. This is significant since in the absence of cooling or heat losses the substrate temperature equals that of the environment eventually⁵⁻⁸.

The synthesis and impurities in TBC materials also influence the stability and life of the coating. Since, the source materials in the present study are minerals like zircon, a silicate of zirconium and rare earth bearing minerals like monazite or bastnasite; precautions were taken to synthesise high purity materials. Over the years, various methods have been investigated to produce feed stock materials like high pure zirconium oxy-chloride and lanthanum chloride from zircon and monazite/bastnasite respectively. However, for the first time the results of TBC material synthesis from these base minerals, their purification, APS grade powder preparation and a high end application being presented comprehensively. Salient aspects of chemical synthesis are outlined here. Also presented is a brief review of implications of having a nano-structured thermal barrier.

1.1 Implications of Nano-structure

Earlier, various methods such as co-precipitation, hydrazine, solution reaction routes, the stearic acid method, alkoxide-based sol-gel and citrate method^{3,5}, sol-gel processing, hydrothermal processing, sonochemical micro emulsion and ion exchange resin manufacture methods⁹ for the preparation of fine and nano-crystalline powders have been investigated^{3,10,11}. The motivation for the nano-structured coating is that the nano- and meso-structured zirconia ceramics combine many desirable properties like low k , high refractive index, high chemical and thermal stability. The wavelength of the reflected light is directly proportional to the particle diameter. Hence TBCs require micro-particles of the order of 1-3 μm to reflect heat in the near IR spectrum. In the medium and far IR bands, larger particles are relevant¹².

Particle size reduction also stabilizes the high-temperature phases at room temperature. It is reported that nano powders, above 20 nm – 30 nm, reverts to monoclinic (m-ZrO₂) phase¹³. The nano material always has a larger thermal expansion coefficient and higher toughness than its micro counterpart. The thermal cycling life of nano LZ is reported to be six times that of micro LZ coatings⁶. The indentation toughness of the nanocrystalline SPPS 7YSZ TBC was found to be five times that of corresponding APS TBC in the most critical in-plane orientation¹⁴. Due to the lower in-plane tensile stress and higher fracture toughness of the nano-composite TBCs, they have higher thermal shock resistance than the conventional TBCs¹⁵. It is reported that the yield stress (τ) and micro-hardness (H_v) of nano-crystalline materials are 2–10 times that of the coarse-grained counterparts of the same composition. Particle size reduction also reduces the flaw sizes in the coating. Therefore the fracture resistance in nano-ceramics is higher compared to conventional micron-sized materials^{16,17}.

Grain boundary scattering, an extrinsic mechanism limiting the thermal conductivity (k), decreases k in nano-crystalline materials. While this may be effective for other ceramics, the thermal conductivity of nano-crystalline stabilised zirconia is unaffected by grain size, even down to 65 nm. The offered explanation that the mean free path of the point defects in YSZ is significantly smaller than even the smallest grain size attainable in nano-crystalline YSZ seems valid¹⁸. Nano-structured TBCs often exhibit excellent performance compared with conventional TBCs such as adhesive strength, thermal shock resistance, thermal insulation, corrosion resistance and so on^{3,19}. A reduced density or more generally, a reduced degree of order is associated with very small nano-particles²⁰, which helps in reducing k . Since Phonons play a major role in heat transport in ceramics, spatial confinement of phonons in nanostructures can strongly affect the phonon spectrum and thus the thermal properties at nano-scale²¹.

The superior thermal shock resistance and thermal cycling capability than conventional TBCs is attributed to the formation of a large number of microcracks, uniformly distributed tiny pores and a large area of nanostructured region with high stress relief capability¹⁴. But the disadvantage is that, one order of magnitude (e.g., from 1 μm to 100 nm) reduction in grain size will enhance sintering rates by up to 4 orders of magnitude. Homogenisation time, which is of the order of

hours in micron sized particles, can be milli-seconds in case of nano-particles²⁰.

In practice, the IR band ranging from 700 nm – 1100 nm, results in heating of the surface if absorbed. Therefore the approach should be to maximize the near IR reflectivity. To achieve the highest near IR reflectivity, the particle size needs to be more than half the heat wavelength that is to be reflected. A comparison of the NIR reflectance of nano and their micro crystalline forms show that the nano-crystalline metal oxides are more reflective, about 15 per cent - 20 per cent higher²². A decrease in mean particle size usually increases the reflectance. Particle size also dictates diffuse reflectance. The reduction in particle size increases the inter particle boundaries and therefore the number of reflections at the boundaries increases. Thus, reflectivity increases at most of the wavelengths when the particle size decrease^{23,24}.

1.2 LZ Advantages

The RE pyrochlores (Re₂Zr₂O₇, Re = La, Gd) are very stable materials even under a reducing atmosphere (APS coating atmosphere for example) and are potential candidates for TBC applications. The structure of ‘La’ and ‘Gd’ zirconates remain stable under reducing atmosphere of Ar(g)/3%H₂(g) at 1400 °C. It is reported that the formation and phase stability of Re₂³⁺Zr₂⁴⁺O₇²⁻ pyrochlores can be attributed to the radius ratio of ions i.e. $r_c = r_{Re} / r_{Zr}$. For $r_c = 1.46$ – 1.78 at standard conditions, pyrochlore structure remains stable whereas fluorite is stable when r_c is less than 1.46. LZ, with an $r_c = 1.61$, can also form at a relatively low temperature⁵. The zirconates with pyrochlore structure, are predominantly cubic and ionic, allow variety of atomic substitutions at the A, B and O sites when the ionic radius and charge neutrality conditions are met. Double-layer coating with La₂Zr₂O₇ as top coat was adopted since it is reported that such a bi-layer coating enhanced the temperature capability of the coating by >100K. LZ also has good chemical compatibility with YSZ at least upto 1250 °C^{1,25-27}. Due to low sintering tendency, the nano-grains could be observed in the coating after thermal cycling⁶. LZ remains stable in a large La/Zr molar ratio range, from 0.87 to 1.15 and remains so even when the La₂O₃ composition changes ± 10 per cent from the stoichiometry^{26,28}. Large amounts of metastable fluorite phase forms during rapid solidification, typical of plasma spray conditions. This fluorite transforms to pyrochlore. This is not critical, since no significant volume change is associated. But, due to the considerably higher vapor pressure of La₂O₃ compared to ZrO₂, the processing of LZ by APS is challenging, resulting in non-stoichiometric coatings. The torch power exerts major influence on the coating stoichiometry. If the gun is operated with hydrogen as secondary plasma gas, as in the present case, the stoichiometry is strongly affected and is well reflected by the lattice parameter. ‘La’ depletion leads to a decrease of the lattice parameter²⁹.

2. SYNTHESIS OF NANO POWDERS

Since chemical synthesis yield microspheres composed of very fine grains^{10,12}, it was preferred in the present work. Also wet chemistry methods provide fascinating alternatives and mixing of species occurs on the atomic scale, thus

producing materials with high compositional homogeneity and stoichiometry control^{3,7,8,11,30}. Weakly agglomerated nanoparticles could be prepared via conventional hydrothermal and molten salts method. However the smallest crystallite size and nano-grains were realised by the alkoxide route⁵. The chemistry of the process used in RE zirconates and cerates influences size of crystallites, crystallisation temperature and powder morphology. Crystallite size of approximately 10 nm, could be synthesised employing the stearic acid and co-precipitation routes⁷. For uniform particle size, care is taken to produce fine particles with lower dispersity. It was observed that stabiliser used in the process influences the particle size uniformity. Stearic and eicosanoic acids resulted better uniformity with standard deviations varying between 5 per cent and 7 per cent¹². The stabiliser used should be easily removed during calcination without leaving behind ionic impurities. Thus, carboxylic acids as stabilizers have a distinct advantage over alkali halide salts.

LZ powders with excellent phase and compositional control via co-precipitation method was obtained and the absence of other precursor ions was validated by ICP-MS. The choice of pH being critical in any co-precipitation process, it was shown that the precipitate be collected beyond pH 10 for obtaining phase-pure LZ³¹. So, in co-precipitation, the hydrolysis reaction is primarily controlled by controlling the pH of precipitation and the rate of addition of the precursor^{7,32,33}. If precursors containing Zr⁴⁺ and La³⁺ ions and a precipitating agent, such as ammonium hydrate, are added in different order, they support different hydrolysis-complex conditions. In one case the reaction occurs initially in an acidic environment and slowly changes to basic, whereas in the reverse order, the reaction occurs in a constant strong basic environment. These differing reactions alter the hydrolysis-complex processes, thereby resulting in changes in morphology, size, crystalline phase and even the chemistry of the final precipitates. Thus, adding chemicals in a different order also affects the product composition and structure. Reaction in acidic environment is not a true co-precipitation process and a mixture of lanthanum hydroxide and zirconium hydroxide results⁷. The powder prepared through co-precipitation is amorphous to X-rays as long as it is calcined below 600 °C. Well defined Raman bands were not observed in the case of the citrate precursor heated to temperatures below 1000 °C. But after calcination at 1200 °C, four of the six Raman bands for LZ were observed³². The scatter was less in co-precipitation route compared to flash combustion and citrate methods. Also LZ prepared through co-precipitation followed by ethanol washing showed much higher surface area compared with the other methods³². The BET values showed that the LZ (A-Alkoxide powder) had lower surface area compared to the LZ (C-Citrate powder) synthesised by the citrate route at 1000 °C. Thus the values of density and surface area are process dependant⁵. The process of preparation has a strong effect on structure, texture and surface properties of the mixed oxides³⁴.

2.1 Crystallisation

The crystallisation temperature (CT) for the LZ powders prepared via co-precipitation was found to be 870 °C from the

thermal analysis^{4,7,31}. As temperature increases, phase transition from fluorite to pyrochlore takes place from 1000 °C onwards and converts fully (100 per cent) to pyrochlore at 1450 °C⁴. The CT depends on the preparation method used, 818 °C for citrate route and 870 °C for alkoxide routes⁵. An exothermic peak in TGA-DTA (without weight loss), denotes crystallisation. The tiny exothermic peak in the DTA at about 1000 °C (1045 °C)⁷ without weight change refers to fluorite-pyrochlore transformation. But during thermal treatments/sintering at high temperatures the nano powders get agglomerated. Few reports indicate the presence of nano grains even after short thermal exposures, which was verified in the present study. The degree of agglomeration, density, the crystallite size and surface area are process dependant^{5,12,13,16,32,34}.

2.2 Impurities

It is well known that, lower the impurity content (namely oxides), higher the stability of YSZ powder. So, oxide impurities need to be controlled. This slows down the phase transformation kinetics. Silica, even at <1 wt. % in YSZ coating, adversely affects the thermal cycling life of the coating. It was found that silica gets segregated especially at grain boundaries triple points where it may lead to local instability²⁶. Taylor et al. found that restricting the total impurity oxides (SiO₂, Al₂O₃, CaO, MgO, TiO₂) content to < 0.15 wt. % in YSZ, delayed the tetragonal to monoclinic transformation⁸. The segregation of deleterious impurities at the bond coat- thermally grown oxide (TGO) interface, makes decohesion at the interface easier. The most deleterious impurity, sulphur, at less than 1/3 monolayer coverage, reduces adhesion by a factor³¹ of 10. In the present research the total oxide impurities content could be restricted to 0.03 per cent maximum (Table 1). The minimum purity of YSZ and LZ obtained are 99.9 per cent and 99.95 per cent, respectively.

3. EXPERIMENTAL PROCEDURE

3.1 Materials and methods

For preparation of LZ, zirconium oxy-chloride is the key starting material produced from Zircon, a natural combination of Zirconia (ZrO₂) and Silica (SiO₂). It is also found concentrated with other heavy minerals e.g., Ilmenite, Rutile, Garnet, Sillimanite, Monazite and Xenotime in beach sand. Zircon is separated from associated heavy minerals as a byproduct while processing through a series of gravity separators followed by a combination of high tension separators, magnetic separators and specific gravity separation devices. Zirconium salt is extracted from zircon by chemical process which includes hydro-metallurgy and solvent extraction process.

Zircon is decomposed by treating with caustic soda at around 600 °C to form a fusion decomposed zircon product which is leached with water to remove easily soluble sodium silicate and filtered to obtain a cake, the zirconium frit. This is treated with hydrochloric acid and filtered to obtain zirconyl chloride solution. Purification of zirconyl chloride and removal of impurities like iron, titanium, silica through basic sulphate process yields a zirconium basic sulphate product with good purity of >99 per cent of zirconium (elemental purity). For high pure zirconium oxy-chloride, the sulphated zirconium

compound is hydrolysed with ammonia and is converted to zirconium hydroxide. Further hydrochloric acid dissolution, purification by solvent extraction using tertiary amine and crystallisation yields a zirconium oxy-chloride product in a very high pure state suitable for TBC application. Zirconium oxy-chloride is converted to zirconium oxy-nitrate and is also used for co-precipitation with lanthanum.

For LZ synthesis, solution of zirconium oxy-nitrate and lanthanum nitrate in distilled water was prepared separately. Both the solutions were then mixed together. The amount of lanthanum in the above solution was such that the final ratio by weight of La_2O_3 to ZrO_2 was 56:41. Following this dissolution, the solution was sprayed to a dilute ammonia solution bath kept under agitation. The bath pH was kept at 8.5 to 9 by adding ammonia. The co-precipitated hydroxide was filtered and thoroughly washed free of nitrates. The gel cake was mixed with 2%w/v poly vinyl alcohol (PVA) and dried slowly at 150 °C for 8 h. The dried cake was crushed and calcined in a furnace at 850 °C for 2 h by maintaining a heating rate of 5 °C/minute. The calcined powder was vibro-screened to eliminate finer fractions to maintain a size range of >20 microns. The synthesis process is depicted in the form of a flowchart as shown in Fig. 1.

3.2 Characterisations

The calcinated powder as analysed using inductively coupled plasma optical emission spectroscopy (ICP-OES-OptimaV) has the following impurities and as shown in Table 1.

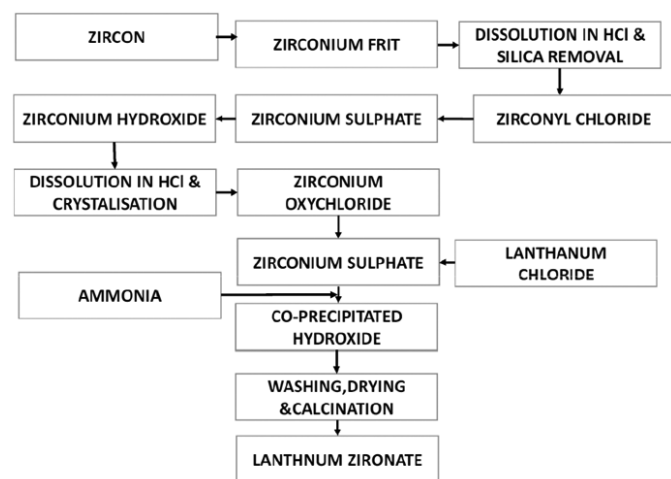


Figure 1. Flow-chart for production of Lanthanum Zirconate.

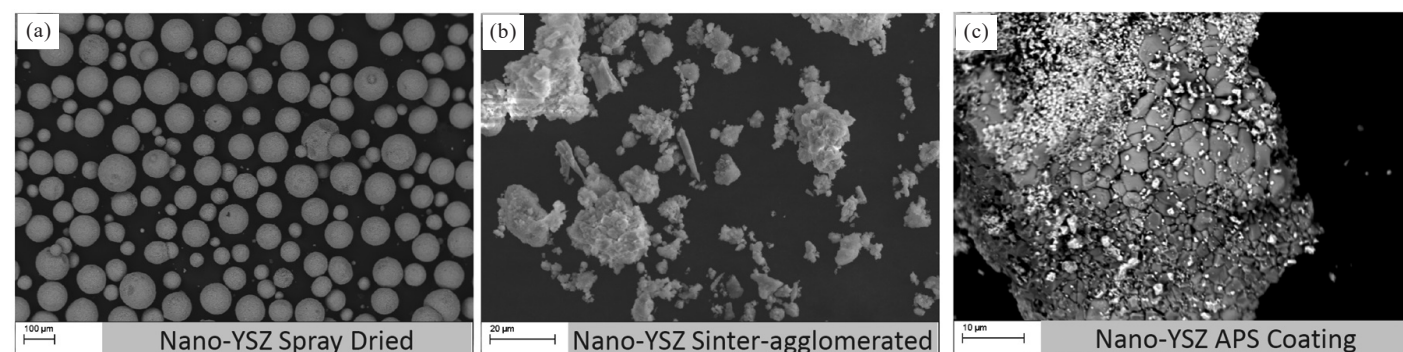


Figure 2. Morphologies of nano powder spray dried, nano powder sinter-agglomerated and powders from coated components.

Table 1. Chemical analysis for impurities in Lanthanum Zirconate prepared by co-precipitation route

Constituents	Value in per centage
Fe_2O_3	<0.003
Al_2O_3	<0.006
TiO_2	<0.005
SiO_2	<0.005
CaO	<0.003
MgO	<0.005
P_2O_5	<0.001

Powder morphology was investigated using SEM (Hitachi Ltd, S-4160). Figure 2 provides a comparison of spray dried, sinter agglomerated nano powders and the coating of spray dried powder. The spray dried nano YSZ powder was made using the sol-gel route for an earlier work. The crystal structure of the YSZ powder, to distinguish cubic and tetragonal phases, was determined by X-ray diffraction. Cu-K_α and Co-K_α radiations were employed both on powders and coated samples. A constant step scanning, with a scan rate $0.2^\circ 2\theta/\text{min}$, was used in the 2θ range of 20–80 degrees. It was observed that both the spray dried nano-powder and its coating contained significant amount of ‘monoclinic’ phase, whereas the indigenised and sinter-agglomerated YSZ powder had either no monoclinic phase or marginal amount (below the detection limit of XRD) Fig. 3.

Thus, the newly synthesised YSZ powder showed maximum amount of ‘tetragonal’- t' phase compared to the other two powder variants. This is due to complete intermixing of species in the atomic scale and the fact that particle size reduction stabilizes the high-temperature modifications. It is this t' structure in YSZ, that is responsible for thermal stability and endurance of the coating^{1,18}. Therefore the content of t' should be as much as possible both in the starting powder & in the coating. The identification of cubic and tetragonal structures, on the basis of X-ray diffraction analysis only, can be erroneous because the lattice parameters of cubic and tetragonal structures are very similar. ($a_o = 0.5124$ nm for cubic, and $a_o = 0.5094$ nm and $c_o = 0.5177$ nm for tetragonal structures). The distinction of tetragonal phase lies in its characteristic peak-splits such as (002) (200), (113) (311), (004) (400), and (006) (600) etc., whereas the cubic phase exhibits only single peaks at all these positions. It was also seen that the chemistry

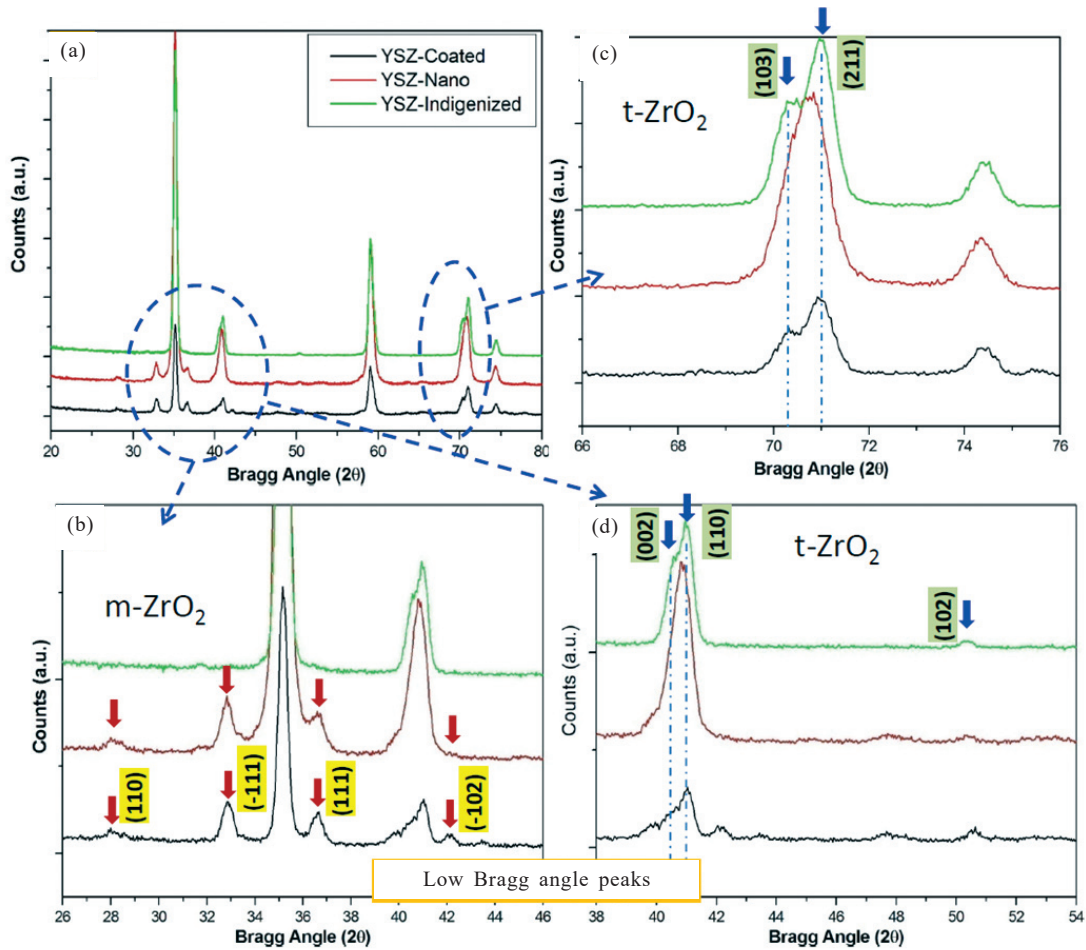


Figure 3. Structure of coated powder (Nano spray dried YSZ), Nano spray dried powder and sintered agglomerated nano powder. Tetragonal structure of the latter is attributed to split peaks (using Co- K α radiation).

of zirconia precursor has a key role in the formation of the crystal structure, polymorphic transformation and crystalline growth.

The LZ powder morphologies, onset of sintering and crystal structure were also studied on the ready to spray LZ powder using TEM-Model Technai-G2 (Fig. 4 and Fig. 5). The spherical shape of the powder can be clearly seen in Figs. 4(a) and 4(c). The onset of sintering and agglomeration is evident in Figs. 4(a), 4(b), and 4(d). This is the condition of the powder after initial calcination at 850 °C for 2 h and preheating at 650 °C for 2 h prior to coating to remove moisture. It is observed that agglomeration and ease of sintering strongly depend on the particle level cleanliness of the powder. Remnants of certain radicals in the powder may act as catalysts in accelerating the sintering process whereas few others may increase sintering resistance. Extensive studies are required in this direction and is beyond the scope of the present work. The SAD pattern in Fig. 5 confirms the fluorite structure which gets converted to pyrochlore upon usage. This is not a cause of concern since fluorite-pyrochlore transition does not involve volume changes which can threaten the coating integrity.

3.3 Thermal Barrier Coating Application

Surface of the component was prepared by grit

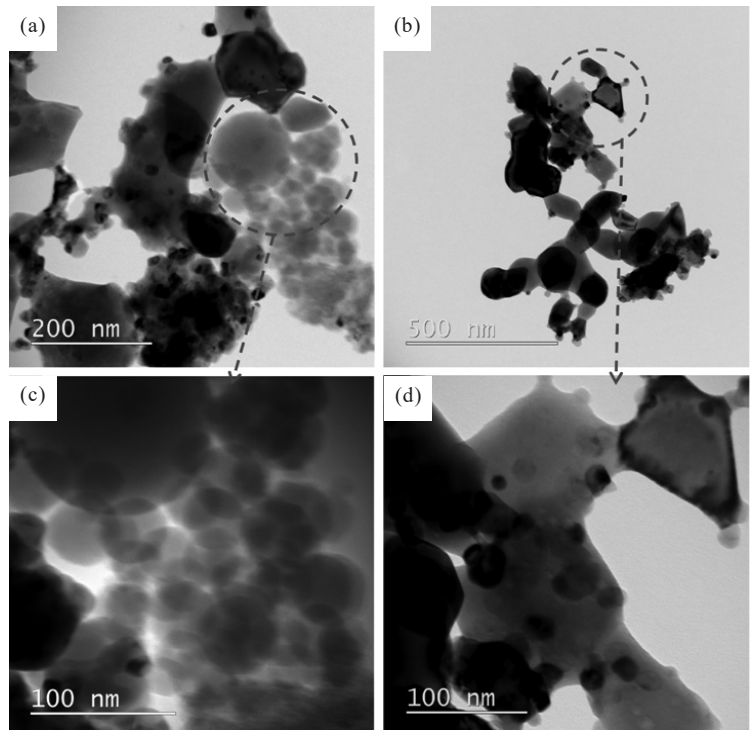


Figure 4. Transmission electron micrographs of sintered LZ powder having size range of 10 nm to 200 nm.

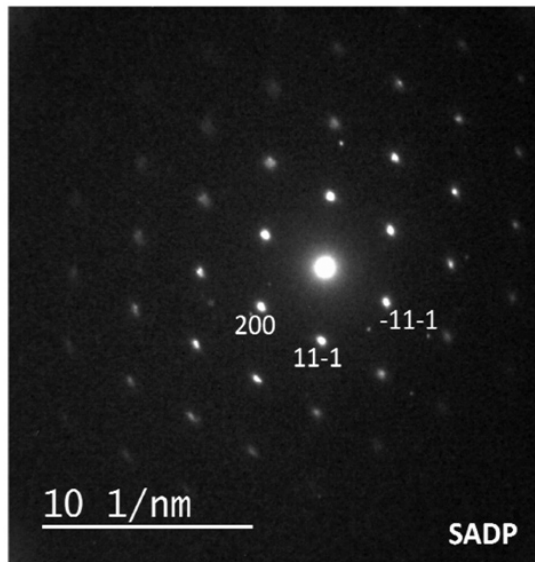


Figure 5. Selected area diffraction pattern (SADP) of sintered LZ powder (ready to spray condition) showing fluorite structure. Zone axis is near [011].

blasting. Synthetic alumina of 120-140 grit sizes were used for the purpose. The calcined and screened powder was air plasma sprayed on to cast Ni-base super alloy substrates and components preliminarily coated with MCrAlY bond coat (Cr 15-19%, Al 5-7%, Y 0.2-0.7%) and less than 50 μm size) and YSZ top coat (thickness 100 μm). LZ was applied (thickness 50 μm - 60 μm) over and above the YSZ to produce a bi-layer TBC. The interruption between YSZ and LZ coatings was kept as low as practicable for better adhesion. The total maximum thickness was kept well below 250 μm . The spray parameters are given in Table 2. Powder feeding disc speed was between 35 per cent - 50 per cent. Temperature measurements on specimens and components after coating, which varied in the range 250 $^{\circ}\text{C}$ - 275 $^{\circ}\text{C}$, was done using hand held IR thermometer IR-L-900. To check the adhesion and quality of the coating on the

specimens (70 mm x 20 mm x 2.5 mm), production bend tests on 10 mm diameter mandrels were done. No visible spalling/delamination was observed upto 60 $^{\circ}$. The bend test was also used to optimise the process parameters. On more ductile substrates, no delamination/spalling was observed upto 90 $^{\circ}$ bending.

Table 2. APS coating parameters

Plasma parameters	MCrAlY bond coat	YSZ coating	LZ coating
Plasma Gun	F4-MB	F4-MB	F4-MB
Current (A)	650	650	675
Voltage (V)	77.5	73.8	74.3
Power (kW)	50.4	47.9	50.2
Primary- Argon (NLPM)	55	55	55
Secondary- Hydrogen (LPM)	13	13	13
Carrier Argon (LPM)	6	5	5
Temperature ($^{\circ}\text{C}$)	3225	3460	3600
Particle velocity (mm/s)	---	243	257
Standoff distance (mm)	100	100	100

4. RESULTS AND DISCUSSION

Figure 6 shows the microstructure of the coated sample. The sample contains small pores on the surface. This is due to the venting of entrapped gases during solidification which is intrinsic to air plasma process. Semi-molten, molten and unmelted regions are also visible. Though the process was not tailored to create vertical cracks in the coating, few vertical cracks are also evident. The estimated density and porosity of the processed coating, according to the Archimedes' method, are 5.40 g/cc and 11 per cent, respectively. After coating, the stoichiometric ratio of $\text{ZrO}_2/\text{La}_2\text{O}_3$ differed from initial composition of the powder due to the evaporation of La_2O_3 in high temperature reducing environment of plasma. This is expected and well reported in literatures. As can be seen

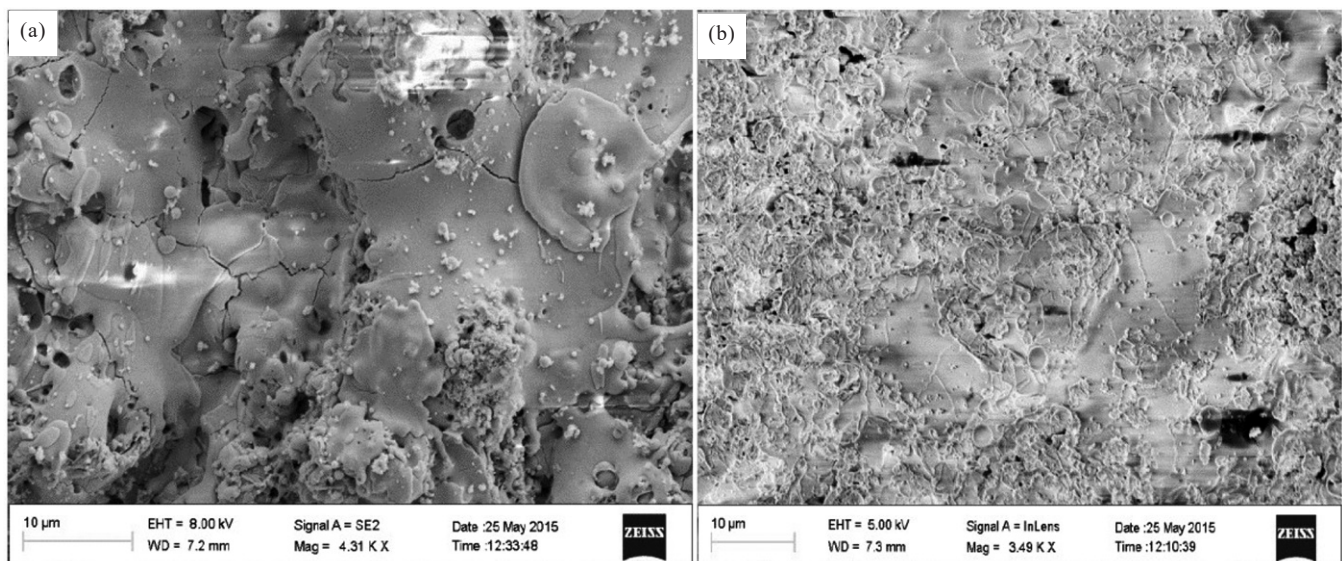


Figure 6. SEM micrograph of the top coat-Lanthanum zirconate. Few cracks are visible on the coating. The coating consists of melted, partially melted and unmelted powders and splats typical to APS.

from the Table 2, the spray current at 675 Amps is also quite high. The semi quantitative results indicate the loss of La_2O_3 (Fig. 7). The higher current was employed to prepare a coating with significant resistance to high velocity gas erosion.

However, as stated, LZ pyrochlore retains its stability even if the La:Zr ratio varies in the range from 0.87 to 1.15. Therefore well defined peaks of cubic pyrochlore are evident in Fig. 8 in spite of La_2O_3 losses during plasma spraying. The coating was examined for the presence of nano-structure using TEM (Fig. 9). The diffraction pattern confirms that the coating consists of nano-particles. Nano structure could be retained in spite of the higher current values than typically employed during such operations. The presence of copper in the spectra is due to the copper grid used in TEM.

The bi-layer YSZ-LZ coated flaps were assembled and tested in an aero-engine which was under accelerated mission testing for long endurance (Fig. 10). The coating withstood rapid thermal transients, supersonic flow of combustion products along with vibratory loads of about 4 'g'. The coating

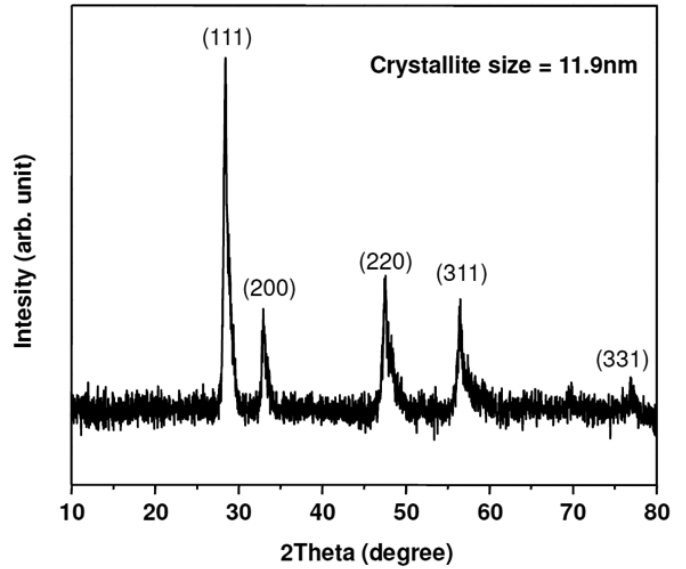


Figure 8. XRD pattern of lanthanum zirconate using Cu- $K\alpha$ radiation: well-defined peaks confirming the presence of cubic- pyrochlore phase of $\text{La}_2\text{Zr}_2\text{O}_7$ (JCPDS card number 73-2363).

sustained 1000 h equivalent of engine operation and more than 30000 nozzle actuations. No chipping off or spallation of the coating was observed as can be seen from Fig. 10. It is also evident that the two flap with indigenous nano structured bi-layer coating have hardly tarnished compared to the other flaps which were coated with commercial YSZ grade. Also the two flap had lesser warpage compared to others which could be due to higher insulation effectiveness of bi-layer coating²⁷. This could be realised right first time due to the application of multiple strategies like nano structures, bi-layer thermal barrier, high purity materials and a thermally stable sinter resistant coating as the top coat among others.

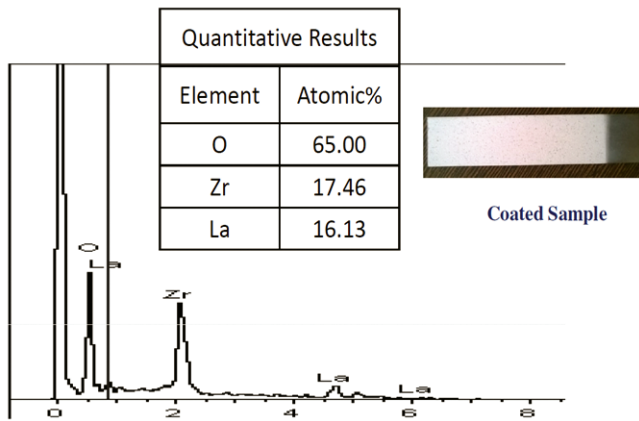


Figure 7. EDS results of Lanthanum zirconate coating, the loss of some lanthanum is evident.

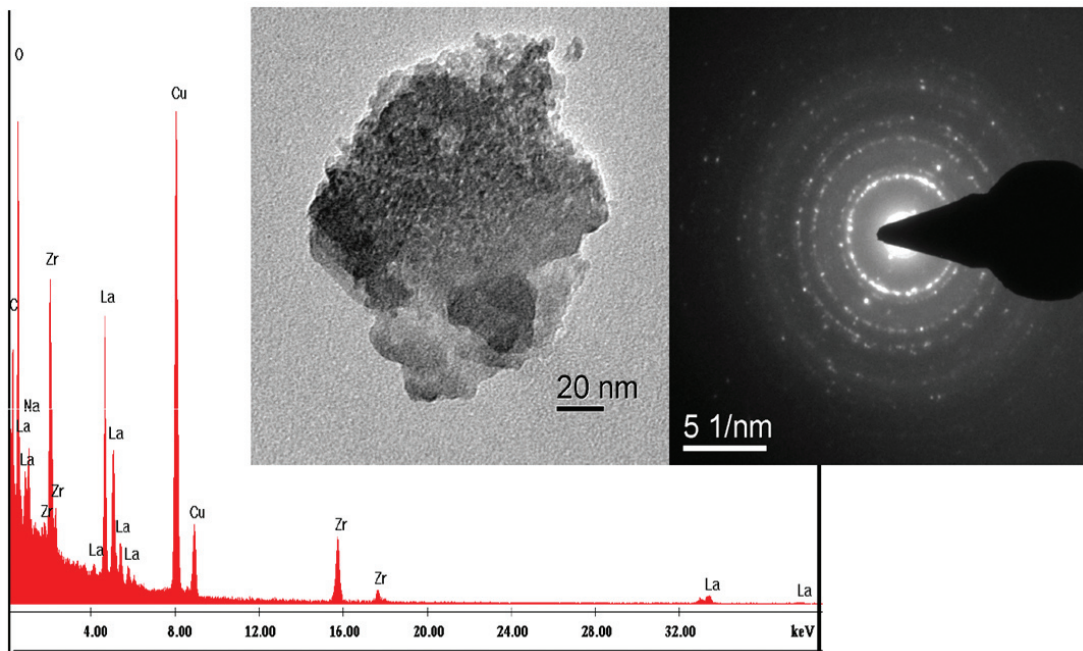


Figure 9. Nano structure of LZ is evident after coating.

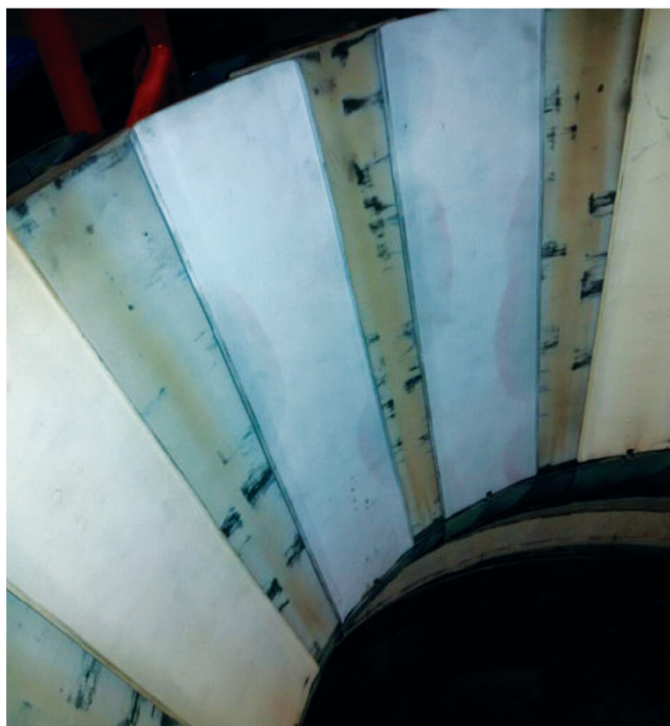


Figure 10. Quality of the improved coating on the two flaps is evident.

5. CONCLUSIONS

Nano structured high purity grade YSZ and LZ could be prepared from beach sand containing monazite and zircon following wet chemical route i.e. co-precipitation method. The sinter-agglomerated powder could be successfully sprayed using APS and a bi-layer TBC was realised. The coating withstood the rigour of aero-engine endurance test. The following conclusions are made.

- (a) Agglomeration of nano powders depends on the process, chemicals used and the degree of washing done during powder preparation.
- (b) The adopted process could ensure very low level of oxide impurities (<0.03 %) which is beneficial to coating stability and life. The present process can be scaled up for bulk production.
- (c) Nano structure could be retained after plasma spraying.
- (d) Fluorite-pyrochlore transition does not affect coating integrity.
- (e) LZ has good long term physico-chemical compatibility with YSZ. The bi-layer coating offers higher thermal insulation and is quite durable.

ACKNOWLEDGEMENTS

The authors like to place on record the unfailing support of IREL, Chhatrapur and HAL, Koraput for providing all the necessary materials and infrastructure for this research.

REFERENCES

1. Liu, X.Y.; Che, J.W.; Yi, H.; Zhang, J. & Liang, G.Y. Diffusion mechanism of oxygen ions in $\text{La}_2\text{Zr}_2\text{O}_7/\text{YSZ}$ composite ceramics. *J. Alloys Compd.*, 2019, **778**, 522-531.

- doi: 10.1016/j.jallcom.2018.11.221
2. Xu, C.; Jin, H.; Zhang, Q.; Huang, C.; Zou, D.; He, F.; & Hou, S. A novel Co-ions complexation method to synthesize pyrochlore $\text{La}_2\text{Zr}_2\text{O}_7$. *J. European Ceramic Society*, 2017, **37**, 2871–2876.
doi: 10.1016/j.jeurceramsoc.2017.02.045
3. Shoja Razavi, A.R. & Loghman-Estarki, M.R. Advance technique for the synthesis of nano-structured zirconia based ceramics for thermal barrier application. *In Sol-gel Based Nanoceramic Materials: Preparation, Properties and Applications*, edited by A.K. Mishra, Springer International Publishing, 2017, pp. 21-91.
doi: 10.1007/978-3-319-49512-5_2
4. Paul, B.; Singh, K.; Jaro, T.; Roy, A. & Chowdhury, A. Structural properties and the Fluorite-Pyrochlore phase transition in $\text{La}_2\text{Zr}_2\text{O}_7$: The role of oxygen to induce local disordered states. *J. Alloys Compd.*, 2016, **686**, 130-136.
doi: 10.1016/j.jallcom.2016.05.347
5. Joulia, A.; Vardelle, M. & Rossignol, S. Synthesis and thermal stability of $\text{Re}_2\text{Zr}_2\text{O}_7$, (Re=La, Gd) and $\text{La}_2(\text{Zr}_{1-x}\text{Ce}_x)_2\text{O}_{7-\delta}$ compounds under reducing and oxidant atmospheres for thermal barrier coatings. *J. Euro. Cer. Soc.*, 2013, **33**, 2633–2644.
doi: 10.1016/j.jeurceramsoc.2013.03.030
6. Xueqiang, C. Application of rare earths in thermal barrier coating materials. *J. Mater. Sci. Technol.*, 2007, **23**(01), 15-35.
7. Chen, H.; Gao, Y.; Liu, Y. & Luo, H. Coprecipitation synthesis and thermal conductivity of $\text{La}_2\text{Zr}_2\text{O}_7$. *J. Alloys Compd.*, 2009, **480**(2), 843–848.
doi: 10.1016/j.jallcom.2009.02.081
8. Kong, L.; Karatchevtseva, I.; Gregg, D.J.; Blackford, M.G.; Holmes, R. & Triani, G. A novel chemical route to prepare $\text{La}_2\text{Zr}_2\text{O}_7$ pyrochlore. *J. Am. Ceram. Soc.*, 2013, **96**(3), 935–941.
doi: 10.1111/jace.12060
9. Geethalakshmi, K.; Prabhakaran, T. & Hemalatha, J. Dielectric studies on nano Zirconium dioxide Synthesized through co-precipitation process. *Int. J. Mater. Metallurgical Eng.*, 2012, **6**(4), 256-259.
10. Chunhui, X.; Hongyun, J.; Qifeng, Z.; Can, H.; Daifeng, Z.; Fujian, H. & Shuen, H. A novel Co-ions complexation method to synthesize pyrochlore $\text{La}_2\text{Zr}_2\text{O}_7$. *J. Euro. Cer. Soc.*, 2017, **37**, 2871–2876.
doi: 10.1016/j.jeurceramsoc.2017.02.045
11. Zhang, Z.; Liu, J.; Wang, F.; Kong, J. & Wang, X. Fabrication of bulk macroporous zirconia by combining sol-gel with calcination processes. *Ceramics International*, 2011, **37**(7), 2549–2553.
doi: 10.1016/j.ceramint.2011.03.054
12. W. Leib, E.; Vainio, U.; M. Pasquarelli, R.; Kus, J.; Czaschke, C.; Walter, N.; Janssen, R.; Müller, M.; Schreyer, A.; Weller, H. & Vossmeier, T. Synthesis and thermal stability of zirconia and yttria-stabilized zirconia microspheres. *J. Colloid Interface Sci.*, 2015, **448**, 582–592.
doi: 10.1016/j.jcis.2015.02.049
13. Davar, F.; Hassankhani, A. & Reza, M. Controllable synthesis of metastable tetragonal zirconia nanocrystals

- using citric acid assisted sol–gel method. *Ceramics International*, 2013, **39** 2933–2941.
doi: 10.1016/j.ceramint.2012.09.067
14. Xianliang, J. Overview on the development of nano-structured thermal barrier coatings. *J. Mater. Sci. Technol.*, 2007, **23**(4), 449–456.
 15. Wang, C.; Wang, Y.; Wang, L.; Hao, G.; Sun, X.; Shan, F. & Zou, Z. Nanocomposite Lanthanum Zirconate thermal barrier coating deposited by suspension plasma spray process. *J. Thermal Spray Technol.*, 2014, **23**(7), 1030–36.
doi: 10.1007/s11666-014-0068-3
 16. Palmero, P. A review of properties and powders' synthesis methods. *Struct. Cer. Nanocompos.: Nanomater.*, 2015, **5**, 656–696.
doi: 10.3390/nano5020656
 17. Mishra, S.K.; Jagdeesh, N. & Pathak, L.C. Fabrication of nanosized Lanthanum Zirconate powder, deposition of thermal barrier coating by plasma spray process. *J. Mater. Eng. Performance*, 2016, **25**(7), 2570–2575.
doi: 10.1007/s11665-016-2122-4
 18. Clarke, D.R. & Levi, C.G. Materials design for the next generation thermal barrier coatings. *Ann. Rev. Mater. Res.*, 2003, **33**, 383–417.
doi: 10.1146/annurev.matsci.33.011403.113718
 19. Wang, L.; Wang, Y.; Sun, X.G.; He, J.Q.; Pan, Z.Y. & Yu, L.L. Preparation and characterization of nanostructured $\text{La}_2\text{Zr}_2\text{O}_7$ feedstock used for plasma spraying. *Powder Technology*, 2011, **212**(1), 267–277.
doi: 10.1016/j.powtec.2011.06.001
 20. Vollath, D. Nanomaterials- An introduction to synthesis, properties and applications. Wiley-VCH Verlag Gmb H & Co, Weinheim, 2008.
 21. Klaus, D.S. Handbook of Nanophysics: Principles and Methods, CRC Press, 2010.
 22. Fang, V.; Kennedy, J.; Futter, J. & Manning, J. A review of near infrared reflectance properties of metal oxide nanostructures. GNS Science Report, 2013, p.39.
 23. Beiswenger, T.N.; Myers, T.L.; Brauer, C.S.; Su, Y.F.; Blake, T.A.; Ertel, A.B.; Tonkyn, R.G.; Szecsody, J.E.; Johnson, T.J.; Smith, M.O. & Lanker, C.L. Experimental effects on IR reflectance spectra: Particle size and morphology. *In Proceedings of SPIE*, 2016, 9840, 01.
doi: 10.1117/12.2223909
 24. Su, Y.F.; Myers, T.L.; Brauer, C.S.; Blake, T.A.; Forland, B.M.; Szecsody, J.E. & Johnson, T.J. Infrared reflectance spectra: Effects of particle size, provenance and preparation. *In Proceedings of SPIE*, 2014, 9253, 04.
doi: 10.1117/12.2069954
 25. Vaßen, R.; Jarligo, M.O.; Steinke, T.; Mack, D.E. & Stover, D. Overview on advanced thermal barrier coatings. *Surface Coatings Technol.*, 2010, **205**(4), 938–942.
doi: 10.1016/j.surfcoat.2010.08.151
 26. Cao, X.Q.; Vassen, R. & Stoeber, D. Ceramic materials for thermal barrier coatings. *J. Euro. Cer. Soc.*, 2004, **24**(1), 1–10.
doi: 10.1016/S0955-2219(03)00129-8
 27. Jing, Z.; Xingye, G.; Yeon, G. J.; Li, L. & James, K. Lanthanum zirconate based thermal barrier coatings: A review. *Surface Coatings Technol.*, 2017, **323**, 18–29.
doi: 10.1016/j.surfcoat.2016.10.019
 28. Xu, Z.; Zhong, X.; Zhang, J.; Zhang, Y.; Cao, X. & He, L. Effects of deposition conditions on composition and thermal cycling life of lanthanum zirconate coatings. *Surface Coatings Technol.*, 2008, **202**(19), 4714–4720.
doi: 10.1016/j.surfcoat.2008.04.046
 29. Mauer, G.; Du, L. & Vaßen, R. Atmospheric plasma spraying of single phase lanthanum zirconate thermal barrier coatings with optimized porosity. *Coatings*, 2016, **6**(4), 49.
doi:10.3390/coatings6040049
 30. Viazzi, C.; Deboni, A.; Ferreira, J.Z.; Bonino, J.P. & Ansart, F. Synthesis of Ytria stabilized Zirconia by sol–gel route: Influence of experimental parameters and large scale production. *Solid State Sci.*, 2006, **8**, 1023–1028.
doi: 10.1016/j.solidstatesciences.2006.02.053.
 31. Kumar, R.; Singh, K.; Chakravarty, D. & Chowdhury, A. Attaining near-theoretical densification in nanograined pyrochlore $\text{La}_2\text{Zr}_2\text{O}_7$ (LZ) ceramic at 1150 °C by spark plasma sintering. *Scripta Mater.*, 2016, **117**, 37–40.
doi: 10.1016/j.scriptamat.2016.02.014
 32. Nair, J.; Nair, P.; Doesburg, E.B.M.; Van-Ommen, J.G.; Ross, J.R.H. & Burggraaf, A.J. Preparation and characterization of Lanthanum Zirconate. *J. Mat. Sci.*, 1998, **33**, 4517–4523.
doi:10.1023/A:1004496100596
 33. Prusty, D.; Pathak, A.; Chintha, A.; Mukherjee, B. & Chowdhury, V. Structural investigations on the compositional anomalies in Lanthanum Zirconate system synthesized by coprecipitation method. *J. Am. Ceram. Soc.*, 2014, **97**(3), 718–724.
doi: 10.1111/jace.12741
 34. Rossignol, S.; Gerard, F. & Duprez, D. Effect of the preparation method on the properties of zirconia–ceria materials. *J. Mater. Chem.*, 1999, **9**, 1615–1620.
doi: 10.1039/A900536F

CONTRIBUTORS

Mr R.K. Satpathy, received his BE (Metallurgy) from REC, Rourkela and MTech (Aircraft Production Engg.) from IIT, Madras. Presently working as Scientist 'G', at DRDO-Defence Metallurgical Research Laboratory, Hyderabad. He has research experience in all facets of gas turbines starting from manufacturing to operations. As a chairman of the Joint Service Specifications (JSS) on coatings, he standardised 15 JSS. He also authored one coating compendium pertaining to aeroengines. In the current study, he is main researcher and primary author.

Dr B.R. Mishra, received his PhD (Chemistry) from Berhampur University, Odisha. Currently working as DGM (R&D) in Indian Rare Earths Limited, Chatrapur. He has industrial experience in the field of process, quality control. He has specialised in solvent extraction process to beach sand heavy minerals like Ilmenite, Zircon and rare earths bearing monazite and Xenotime. Has five patents to his credit. In the current study, he did raw materials and TBC material synthesis.

Mr B. Mallick, Chief Manager –Indigenisation, Hindustan Aeronautics Limited, Koraput. He has received his ME in Mechanical Engineering from REC Rourkela in 1995. Earlier he worked as structural design engineer in aviation gas turbine and thermo gas dynamics and performance engineer. He has contributed immensely to indigenisation of compressor and turbine blades of helicopter and transport aircraft engines. In the current study, he did APS Coating studies and coating qualifications support.

Prof. B.K. Mishra, is graduated in Metallurgy from NIT Rourkela, and received PhD from University of Utah, USA. Presently working as Director *Indian Institute of Technology, Goa*. Has published over 240 research papers in minerals, materials, and environmental engineering area. He is the recipient of the National Geoscience Award and is a fellow of the INAE. For his contribution to industrial R&D he received the most coveted VASVIK Award and CSIR Technology Award (team award).

In the current study, he did research guidance and support.